Unizik Journal of Technology, Production and Mechanical Systems (UJTPMS)

journal homepage: https://journals.unizik.edu.ng/index.php/ujtpms/about
PRINT ISSN: 1115-7143 || ONLINE ISSN: 1115-7453

Evaluation of Carbonized Hamburger Seed Shells for Methylene Blue Dye Removal: Adsorption Efficiency and Dose-Response Analysis

Godspower Onyekachukwu Ekwueme [1*], Orobosa Kingsley Osazuwa[2], Chukwunedum Ogochukwu Chinedum[3]

[1] Department of Industrial Production Engineering, Nnamdi Azikiwe University, Awka, Anambra State, 420102, NIGERIA
[2] Department of Mechanical Engineering, Nnamdi Azikiwe University, Awka, Anambra State, 420102, NIGERIA
[3] Department of Industrial Production Engineering, Nnamdi Azikiwe University, Awka, Anambra State, 420102, NIGERIA

ARTICLE INFO

Article history:
Received February. 18, 2025
Revised March 20, 2025
Accepted March 25, 2025

Available online March. 28, 2025

Keywords:
Adsorption efficiency, Methylene blue dye, Dose-response analysis, pH optimization, KOH activation, Pseudo-second-order model, Wastewater treatment

ABSTRACT

This study evaluates the adsorption efficiency of carbonized and potassium hydroxide (KOH), activated hamburger seed shells (CPAHS) for methylene blue dye removal from aqueous solutions. The adsorbent was characterized for surface area, fixed carbon content, ash content, volatile matter, and functional groups to determine its suitability for adsorption applications. The data employed in this study was primary data obtained from experimental methods, which involved gathering, preparing, and analysing chemicals and raw materials in a laboratory. To evaluate the impact of pH, adsorbent dosage, initial dye concentration, and contact time on removal efficiency, batch adsorption studies were carried out. Fourier Transform Infrared Spectroscopy (FTIR) and Scanning Electron Microscopy (SEM) were employed to analyze the functional groups and surface morphology of CPAHS. Results indicated that CPAHS exhibited a high surface area (400.9–548.6 m^2/g) and significant adsorption capacity, with the optimal pH for dye removal identified between 6 and 8. The adsorption process was analyzed using a four-parameter log-logistic function, with dose-response modelling revealing an Effective Dose $(ED)_{50}$ value indicative of efficient adsorption at moderate CPAHS concentrations. The adsorption kinetics followed the pseudo-second-order model, suggesting a chemisorption-dominated mechanism. Furthermore, a first-order decay model demonstrated that dye concentration reduction was most rapid at near-neutral pH levels. These findings highlight the potential of CPAHS as a cost-effective and environmentally sustainable adsorbent for dye-contaminated wastewater treatment. The study underscores the value of utilizing agro-waste materials for pollutant removal, contributing to both waste management and water purification efforts.

1. Introduction

Industrial wastewater, particularly from the textile, dyeing, and paper industries, has emerged as a significant environmental concern due to its complex composition and hazardous nature. The increasing production and use of synthetic dyes in industrial applications have resulted in large volumes of dye-contaminated wastewater being discharged into aquatic environments, causing severe ecological and human health risks [1]. Many of these dyes exhibit high chemical stability, making them resistant to natural degradation and conventional wastewater treatment techniques [2]. Dye pollutants in water bodies pose multiple challenges. Firstly, their high visibility alters the aesthetic quality of water resources, reducing their usability for domestic and industrial purposes. Secondly, dyes absorb and reflect sunlight, thereby interfering with aquatic photosynthesis, which is crucial for maintaining oxygen levels in water bodies [3-4]. Furthermore, many synthetic dyes contain carcinogenic and mutagenic compounds that threaten aquatic life and human health through bioaccumulation in the food chain [5]. Therefore, developing efficient, cost-effective, and

*Corresponding author: og.ekwueme@unizik.edu.ng

sustainable techniques for removing dyes from industrial wastewater is imperative to mitigate pollution and protect aquatic ecosystems.

Over the years, several techniques have been explored for dye removal, including chemical oxidation, membrane filtration, coagulation-flocculation, biological treatment, and adsorption [2]. Of these, adsorption has drawn a lot of interest because of its great effectiveness, ease of use, and capacity to eliminate a variety of organic contaminants, including stubborn dyes [6]. The process involves the adherence of dye molecules to the surface of an adsorbent, thereby eliminating them from the aqueous phase. Activated carbon is the most widely used adsorbent in industrial wastewater treatment due to its high surface area, well-developed porosity, and excellent adsorption properties [7]. However, commercially produced activated carbon remains expensive, and its regeneration poses economic and environmental challenges. The disposal of spent activated carbon can lead to secondary pollution, making it necessary to explore alternative low-cost and sustainable adsorbents [8]. This has led to a growing interest in agricultural waste materials as precursors for activated carbon production.

Several studies have investigated the potential of biomass-based activated carbons derived from agricultural residues, including coconut shells, rice husks, sawdust, and lignite [9-10]. The high carbon content of these materials makes them promising alternatives to conventional activated carbon. Ajala et al. [11] explored the use of hamburger seed coat waste to produce activated charcoal using zinc chloride activation, demonstrating high porosity and pollutant removal efficiency comparable to commercial charcoal. Similarly, [12] investigated Cr (VI) adsorption using activated carbon from Ethiopian lignite, achieving 98% removal efficiency at pH 1, with adsorption following Freundlich isotherm and second-order kinetics. Mousavi et al. (2022) optimized methylene blue adsorption using activated carbon from grape leaves, achieving 97.4% removal efficiency at pH 11 and 12.5 g/L dosage, following the Langmuir isotherm and pseudo-second-order kinetics. Additional studies have explored the adsorption potential of other low-cost materials, such as Ethiopian kaolin clay for different dyes [13], eggshell powder for methyl red removal [15], polymeric composite grafted on eggshells for methylene blue removal [14], and calix[6]arene-modified PbS as a regenerative adsorbent for methylene blue [16]. These studies highlight the viability of alternative adsorbents for wastewater treatment.

Despite the growing interest in biomass-derived adsorbents, certain research gaps remain. While [11] demonstrated the adsorption potential of hamburger seed shells, there is a lack of comprehensive research on their adsorption kinetics, isotherms, and thermodynamics, particularly for methylene blue dye removal. Many studies focus on batch adsorption studies but do not quantitatively analyze dose-response relationships using advanced modelling techniques. Understanding how adsorbent dosage influences dye removal efficiency through mathematical modelling remains underexplored. Most studies focus on single-use adsorption without investigating the regeneration potential of biomass-based activated carbon, which is crucial for economic and environmental sustainability. Addressing these research gaps will contribute to the existing body of knowledge and provide practical insights into the application of carbonized hamburger seed shells as an effective and sustainable adsorbent for wastewater treatment.

Hence, this study aims to evaluate the adsorption efficiency and dose-response characteristics of carbonized hamburger seed shells (CPAHS) for methylene blue dye removal. The key objectives include: Determining the surface area, fixed carbon content, ash content, volatile matter, and functional groups of CPAHS to assess its suitability for adsorption applications; Investigate how different pH levels (acidic, neutral, and alkaline) influence the adsorption of methylene blue, identifying the optimal pH conditions for maximum removal efficiency; Evaluate the relationship between CPAHS dosage and dye removal efficiency, highlighting the optimal dosage for effective adsorption while avoiding diminishing returns; Apply a four-parameter log-logistic function to characterize the dose-response behaviour of CPAHS, identifying key parameters such as ED50 (effective dose for 50% removal), upper asymptote, and slope to quantify adsorption performance; Use pseudo-first-order and pseudo-second-order kinetic models, as well as Langmuir and Freundlich isotherms, to understand adsorption mechanisms and capacity; and Use a first-order decay model to determine the rate constants of dye concentration reduction under varying pH conditions, establishing the most effective pH for rapid dye degradation. By addressing these objectives, the study will contribute to the development of cost-effective and sustainable adsorbents for wastewater treatment. The findings will enhance the understanding of adsorption mechanisms, provide a mathematical basis for dose-response relationships, and support the practical application of CPAHS in industrial wastewater treatment.

2. Materials and Methods

2.1 Source of Data

The data used in this research were primarily experimental, and obtained through laboratory-based procedures involving the collection, preparation, and analysis of raw materials and chemicals. The data sources are categorized into primary data, gathered from field collection and laboratory experiments.

2.2 Raw Material and Equipment

1. Hamburger seed shell
2. Furnace
3. Distilled water
4. Potassium hydroxide (KOH)
5. Crusher
6. Dryer
7. Sieve.

2.2.1 Sample Collection and Preparation

A large number of hamburger seed shells were obtained from waste basket sites within the Afia nine market, Enugu. The collected samples were deseeded to remove some particles of hamburger seed. The shell was initially washed thoroughly with potable water to remove dust, colour, and impurities then rinsed with distilled water and oven dried at 110 ^{o}C for 3 hours. After this, the samples were grounded and screened using a mesh size of 3.5mm. The obtained samples were stored for the carbonization process.

2.2.2 Adsorbate

Methylene blue dye commonly known as methylene blue dye is a basic dye with a molecular weight of 319.9 and an empirical formula of $C_{16}H_{18}N_3SCl$. It is the most commonly used substance for dying cotton, wood, leather and silk [17]. It is a basic dye that is typically cationic or positively charged and reacts well with a material that is anionic or negatively charged. Methylene blue dye was chosen in this study because of its known strong adsorption onto solids

.

2.2.3 Carbonization Process

The raw hamburger seed shells were carbonized to prepare activated carbon. The shells were screened, placed into a platinum crucible, and transferred to a muffle furnace (Carbolite Sheffield England LMF4) under a limited air supply. Carbonization was conducted at 800°C for 2 hours. After cooling to room temperature, the carbonized sample was weighed and stored for subsequent activation.

2.2.4 Activation Process

To enhance adsorption properties, the carbonized material underwent chemical activation using potassium hydroxide (KOH) following a conventional activation approach. The carbonized sample and KOH were mixed in a 1:1.5 weight ratio to form a slurry. The mixture was stirred thoroughly, placed in a muffle furnace at 850°C for 1 hour, and then cooled to room temperature.

The resulting activated carbon was crushed, washed with hydrochloric acid (HCl) and distilled water until a neutral pH (6–7) was achieved, and oven-dried. The yield was calculated as the ratio of the weight of dried activated carbon to the initial weight of the carbonized sample.

2.2.5 Preparation of Methylene Blue Dye Stock Solution

A 1000 mg/L stock solution of methylene blue dye was prepared by dissolving 1 g of dye in distilled water, with the final volume adjusted to 1 L in a volumetric flask. The solution was homogenized by shaking and stored for serial dilutions. Dye concentrations were analyzed spectrophotometrically at 668 nm following the procedure of [18].

2.2.6 Characterization of Activated Carbon

i. Fourier Transform Infrared Spectroscopy (FTIR)

FTIR analysis was performed using a Buck 530 IR spectrometer to identify surface functional groups within the wavelength range of **600–4000 cm^{-1}**.

ii. Scanning Electron Microscopy (SEM)

The surface morphology of the raw and activated materials was examined using a Phenom ProX SEM (PhenomWorld, Eindhoven, Netherlands).

iii. Surface Acidity and Basicity

Surface acidity and basicity were measured following the methods of [19] by titration with 0.05 M NaOH and HCl, respectively.

iv. pH of Point of Zero Charge (pHpzc)

Determination was conducted using the solid addition method [20], variations in initial and final pH values were recorded to determine the pHpzc.

v. Moisture Content and Ash Content

Moisture content was determined via thermal drying at **105°C** [21]. Ash content was quantified by incinerating the sample in a muffle furnace at **650°C** for 3 hours until a constant weight was achieved.

vii. Fixed Carbon Content and Bulk Density

Fixed carbon was estimated by subtracting the percentages of volatile matter, ash, and moisture from 100. Bulk density was measured using the method described by [22], involving a graduated cylinder and precise weighing.

2.2.7 Batch Adsorption Studies

Adsorption studies were conducted using 200 mg of activated carbon with methylene blue dye solutions of varying concentrations (100–400 mg/L). Adsorption was allowed to reach equilibrium over 24 hours, followed by washing and drying the adsorbent. The percentage removal of methylene blue was calculated using the equation:

$$\%Removal = \frac{(C_0 - C_t)}{C_0} \times 100 \quad (1)$$

Where C_0 andC_t represents the initial and equilibrium concentrations of the dye, respectively.

2.2.8 Adsorption Parameters Investigated

i. **Effect of pH**
Adsorption was studied at different pH levels (2–10) using 0.1 M HCl and NaOH.

ii. **Effect of Dosage**
Adsorbent dosages ranging from **0.05g to 0.2g** were tested, keeping other parameters constant.

iii. **Effect of Time**
The adsorption process was monitored over varying time intervals at a constant temperature of **303K**.

iv. **Effect of Initial Concentration**
Adsorption efficiency was evaluated for dye concentrations between **50mg/L and 180 mg/L**.

2.2.9 Adsorption Kinetic Models

Adsorption kinetics were analyzed using the following models:

i.**Pseudo-First-Order Model** (Lagergren model)

$$\log(q_e - q_t) = \log q_e - \frac{k_1}{2.303} t \quad (2)$$

Where q_e represents the equilibrium adsorption capacity (amount of adsorbate per unit mass of adsorbent at equilibrium), q_t represents the adsorption capacity at any time *t* (amount of adsorbate adsorbed per unit mass of adsorbent at time *t*), k_1 represents the pseudo-first-order rate constant, which describes the speed of the adsorption process, and t represents the time during which adsorption is occurring

ii.**Pseudo-Second-Order Model**

Based on chemisorption principles, the model evaluated adsorption rates as a function of equilibrium capacity.

This section has detailed the methodology employed in the preparation, characterization, and application of activated carbon derived from hamburger seed shells for the adsorption of methylene blue dye. The study utilized a systematic approach to converting agricultural waste into a value-added adsorbent through a series of well-structured processes, including carbonization, chemical activation, and characterization. The methods presented demonstrate an effective utilization of agro-waste for producing adsorbents with significant potential in wastewater treatment applications.

.

3. Results and Discussion

This section evaluates the characteristic properties of activated carbon from hamburger seed shells, focusing on its potential for methylene blue dye adsorption efficiency and capacity.

3.1 Characteristic Properties of Conventional Activated Carbon from Hamburger Seed Shell (CPAHS)

The properties of activated carbon prepared from hamburger seed shells (CPAHS) were evaluated to determine its suitability for methylene blue dye adsorption. It was found that the value of the Surface Area ranges from 400.9 to 548.6 m²/g, indicating a relatively high surface area. The iodine Number was found to range from 660.8 to 1009.3 mg I_2/g, suggesting good adsorption capacity. The Moisture Content was low, varying between 3.2% and 4.0%, which is beneficial for adsorption efficiency. Ash Content was between 3.2% and 6.0%, with lower ash content favourable for higher adsorption capacity. Volatile Matter values range from 2.2% to 3.6%, indicating stable material.

Fixed Carbon was found to have high fixed carbon content (88.5% to 89.7%), suggesting strong carbonization. The pH was near neutral, with values between 6.8 and 7.1, which may be advantageous for dye adsorption.
While the Bulk Density was approximately 0.48 to 0.51 g/ml, implying good packing density.

3.2 FTIR Analysis of Raw Hamburger Seed Shell

FTIR spectroscopy revealed various functional groups in raw hamburger seed shell, indicating potential adsorption sites for dye molecules:
Alkenes: =C-H bend at 672.5 cm^{-1} (medium to strong intensity).
Alkyl Halides: C-Cl and C-F stretches at 773.3 cm^{-1} and 1008.6-1140.9 cm^{-1}, respectively.
Methyl Groups: C-H bending at 1438.7 cm^{-1}.
Nitro Compounds: N-O symmetric stretching at 1364.1 cm^{-1}.
Carbonyl Compounds: C=O stretches (ketones and acyl chlorides) around 1678.6 and 1794.6 cm^{-1}.
Carboxylic Acids: Broad O-H stretches from 2531.0 to 3385.3 cm^{-1}, contributing to dye binding sites.
Water Molecules: O-H stretches between 3549.2 and 3804.0 cm^{-1}, showing the presence of adsorbed water. This result highlights the presence of polar and non-polar functional groups, which contribute to the adsorptive capacity of CPAHS, making it suitable for methylene blue dye treatment.

Table 1- Summary of the effect of pH Levels on Final Concentrations for 50 mg/L and 80 mg/L Initial Concentrations

pH	**50mg/L**	**80mg/L**
pH_2	7.9440	14.2032
pH_4	2.5000	4.4000
pH_6	1.9020	3.2150
pH_8	1.1000	2.0828
pH_{10}	1.6232	1.8456

The results in Table 1 indicate a clear trend in the effect of pH levels on the final concentrations of the substance for both 50 mg/L and 80 mg/L initial concentrations. At pH 2, the highest final concentrations were recorded (7.9440 mg/L for 50 mg/L and 14.2032 mg/L for 80 mg/L), suggesting minimal removal efficiency at highly acidic conditions. As the pH increased, the final concentrations decreased, demonstrating improved removal efficiency. At pH 4, the concentrations dropped significantly to 2.5000 mg/L and 4.4000 mg/L, respectively. A further decrease was observed at pH 6 (1.9020 mg/L and 3.2150 mg/L), with the lowest concentrations occurring at pH 8, where only 1.1000 mg/L and 2.0828 mg/L remained in solution. Interestingly, at pH 10, there was a slight increase in concentration (1.6232 mg/L and 1.8456 mg/L), indicating a potential reduction in removal efficiency at highly alkaline conditions. Moreover, the data suggest that the optimal pH for reducing final concentrations lies between pH 6 and pH 8, where the removal process is most effective.

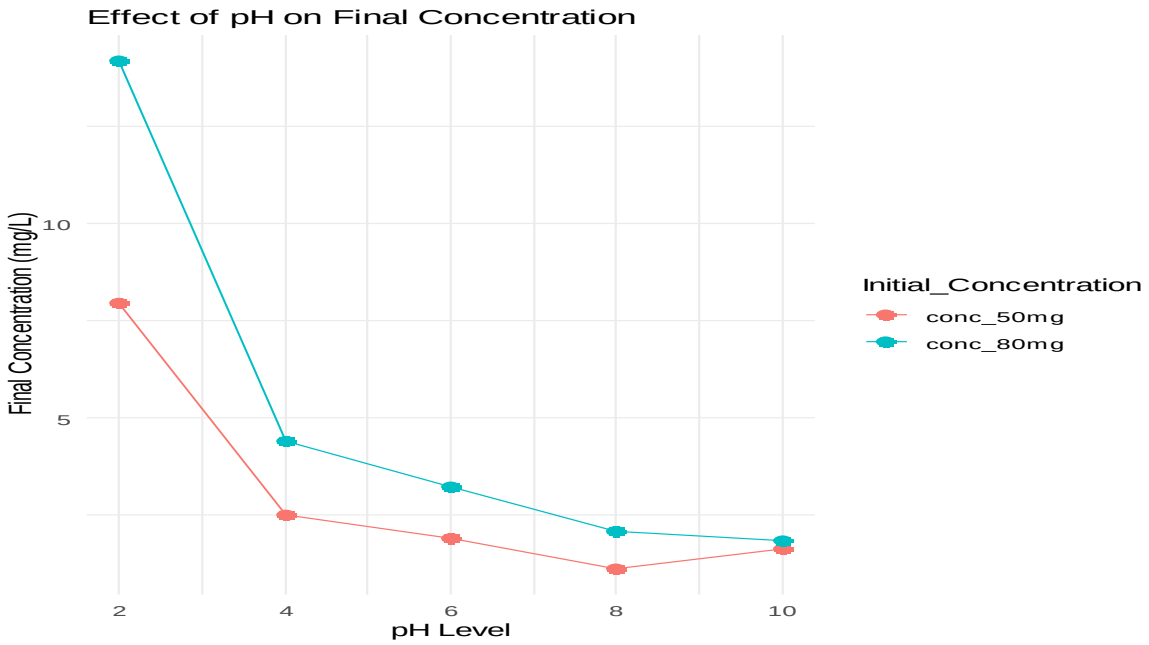

Fig. 1.-Graph of pH Levels on Final Concentrations for 50 mg/L and 80 mg/L Initial Concentrations

The results presented in Fig. 1 illustrate the effect of pH levels on the final concentrations for initial concentrations of 50 mg/L and 80 mg/L. The general trend shows a sharp decline in final concentration as pH increases from 2 to 8, followed by a slight increase at pH 10. At pH 2, the highest final concentrations were observed (7.944 mg/L for 50 mg/L and 14.2032 mg/L for 80 mg/L), indicating poor removal efficiency under highly acidic conditions. As pH increased to 4, the concentrations significantly dropped to 2.500 mg/L and 4.400 mg/L, respectively. The lowest concentrations were recorded at pH 8, where the final values reached 1.100 mg/L and 2.0828 mg/L, suggesting the optimal pH range for maximum removal efficiency. However, at pH 10, the final concentrations slightly increased (1.6232 mg/L for 50 mg/L and 1.8456 mg/L for 80 mg/L), indicating a possible decline in removal efficiency in highly alkaline conditions. This trend suggests that pH plays a crucial role in the removal process, with optimal performance occurring between pH 6 and pH 8.

Table 2-Summary of the effect of Dosage on Final Concentrations at Varying Initial Concentrations (Mg/L)

Dosage	**50mg/L**	**80mg/L**	**110mg/L**
0.02	0.6232	0.8456	3.8163
0.05	0.5128	0.7881	2.099
0.08	0.4640	0.6842	1.6273
0.11	0.3211	0.5900	1.2866
0.14	0.2920	0.5530	1.3935
0.17	0.2700	0.5100	1.3522
0.20	0.2522	0.4823	1.3220

Table 2 presents the effect of dosage on the final concentrations at varying initial concentrations (50 mg/L, 80 mg/L, and 110 mg/L). The results indicate that as the dosage increases from 0.02 g to 0.20 g, the final concentrations decrease, demonstrating improved removal efficiency with higher dosages. For an initial concentration of 50 mg/L, the final concentration drops from 0.6232 mg/L at 0.02 g dosage to 0.2522 mg/L at 0.20 g. Similarly, for 80 mg/L, the concentration reduces from 0.8456 mg/L to 0.4823 mg/L, while for 110 mg/L, it declines from 3.8163 mg/L to 1.3220 mg/L. The most significant reductions are observed at lower dosages, particularly from 0.02 g to 0.11 g, beyond which the decrease in concentration becomes more gradual. Also, at higher dosages (0.14 g – 0.20 g), the final concentrations for 110 mg/L show slight fluctuations (1.3935 mg/L at 0.14 g, then 1.3220 mg/L at 0.20 g), suggesting a saturation point where increasing dosage yields minimal additional removal. This trend suggests that while increasing dosage enhances removal efficiency, there exists an optimal range beyond which additional dosage provides diminishing returns.

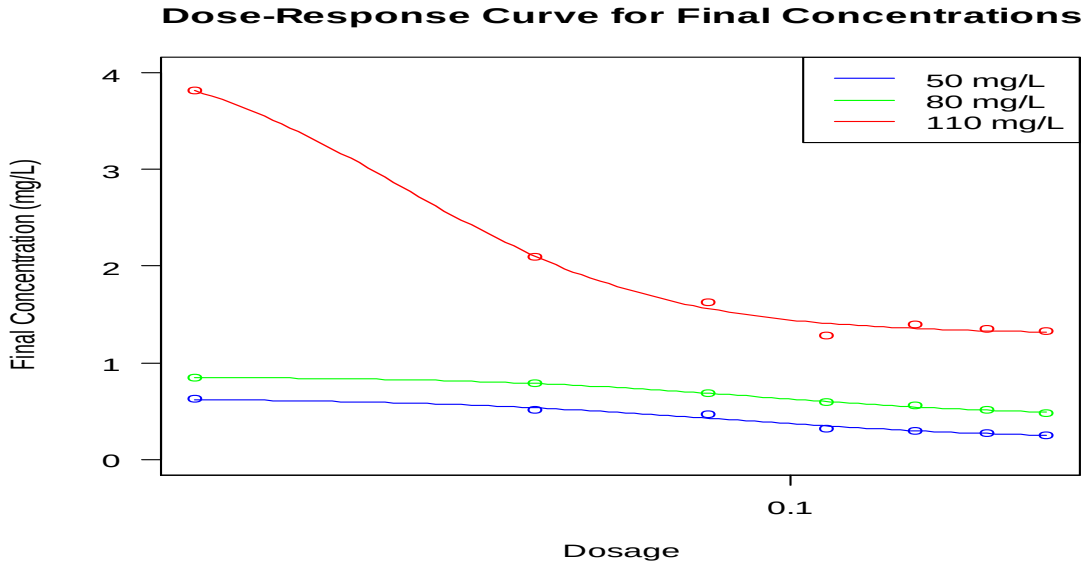

Fig. 2-Graph of Dosage on Final Concentrations at Varying Initial Concentrations (Mg/L)

Fig. 2 illustrates the effect of dosage on final concentrations for varying initial concentrations (50 mg/L, 80 mg/L, and 110 mg/L). The graph shows a general decreasing trend, indicating that higher dosages lead to lower final concentrations, improving removal efficiency. The steepest decline is observed for 110 mg/L, where the final concentration decreases from approximately 3.8163 mg/L at 0.02 g to around 1.3220 mg/L at 0.20 g, suggesting a significant adsorption effect. Similarly, for 80 mg/L, the concentration drops from 0.8456 mg/L to 0.4823 mg/L, while for 50 mg/L, it decreases from 0.6232 mg/L to 0.2522 mg/L. The curve for 110 mg/L shows the most pronounced drop, indicating that higher initial concentrations benefit more from increased dosages. However, at higher dosages beyond 0.14 g, the reduction in concentration becomes less significant, implying a saturation point. This suggests that while increasing dosage enhances removal, there is an optimal dosage beyond which additional increases provide diminishing returns.

Table 3-Model fitted for Conc_50mg: Log-logistic (ED50 as parameter) (4 parms)

Parameter estimates	Estimate	Std.Error	*t*-value	*p*-value	
***b*:(Intercept)**	2.3975	1.1601	2.0666	0.1306	
***c*:(Intercept)**	0.1990	0.0790	2.5193	0.0862	.
***d*:(Intercept)**	0.6307	0.0483	13.0372	0.0009	***
***e*:(Intercept)**	0.0839	0.0141	5.9361	0.0095	**

Signif. codes: 0 '***' 0.001 '**' 0.01 '*' 0.05 '.' 0.1 ' ' 1
Residual standard error: 0.0293 (3 degrees of freedom)

The result presented in Table 3 shows the result of the log-logistic dose-response model that was fitted to the Conc 50mg data, where ED50 is the parameter of interest. The model was specified with four parameters (*b, c, d, e*), and the coefficients and their statistical significance are reported. The log-logistic model used has four parameters:
b (Intercept): Represents a shift in the dose-response curve.
c (Intercept): Related to the slope or shape of the curve.
d (Intercept): Controls the upper asymptote (maximum effect) of the curve.
e (Intercept): Controls the lower asymptote or baseline effect.

The d parameter (0.6307, $p = 0.0009$*) is highly significant ($p < 0.001$), indicating a strong effect on the model, while the e parameter (0.0839, $p = 0.0095$) is also statistically significant ($p < 0.01$), suggesting it plays a crucial role in defining the dose-response relationship. However, the b (2.3975, $p = 0.1306$) and c (0.1990, $p = 0.0862$) parameters are not statistically significant at the 0.05 level, implying weaker contributions to the model. The residual standard error is 0.0293 with 3 degrees of freedom, indicating a good model fit. The results suggest that the log-logistic function adequately describes the relationship between dosage and final concentration at 50 mg/L, with d and e being the most influential parameters.

Table 4- Model fitted for Conc_80mg: Log-logistic (ED50 as parameter) (4 parms)

Parameter estimates	Estimate	Std.Error	t-value	*p*-value	
***b*:(Intercept)**	2.6468	0.3541	7.4744	0.0049	**
***c*:(Intercept)**	0.4407	0.0242	18.1450	0.0003	***
***d*:(Intercept)**	0.8542	0.0109	78.1392	4.6E-06	***
***e*:(Intercept)**	0.0916	0.0049	18.6797	0.0003	***

Signif. codes: 0 '***' 0.001 '**' 0.01 '*' 0.05 '.' 0.1 ' ' 1
Residual standard error: 0.0086 (3 degrees of freedom)

Table 4 presents the parameter estimates for the Log-logistic model fitted to Conc_80mg, using ED50 as a parameter with four estimated parameters (b, c, d, and e). The results indicate that all parameters are statistically significant. The d parameter (0.8542, $p = 4.6E\text{-}06$*) is highly significant ($p < 0.001$) and has the highest t-value (78.1392), suggesting it has the strongest effect on the model. Similarly, the c (0.4407, $p = 0.0003$*) and e (0.0916, $p = 0.0003$*) parameters are also highly significant, reinforcing their importance in defining the dose-response relationship. The b parameter (2.6468, $p = 0.0049$) is statistically significant at $p < 0.01$, indicating a strong contribution. The residual standard error is 0.0086 with 3 degrees of freedom, suggesting an excellent model fit with minimal deviation. These results confirm that the log-logistic function effectively models the relationship between dosage and final concentration at 80 mg/L, with d and e playing crucial roles in the response pattern.

Table 5- Model fitted for Conc_110mg: Log-logistic (ED50 as parameter) (4 parms)

Parameter estimates	Estimate	Std.Error	t-value	*p*-value	
***b*:(Intercept)**	2.8369	1.0330	2.7461	0.0709	.
***c*:(Intercept)**	1.2953	0.0777	16.6567	0.0004	***
***d*:(Intercept)**	4.3268	0.6493	6.6631	0.0068	**
***e*:(Intercept)**	0.0351	0.0080	4.3454	0.0225	*

Signif. codes: 0 '***' 0.001 '**' 0.01 '*' 0.05 '.' 0.1 ' ' 1
Residual standard error: 0.0846 (3 degrees of freedom)

Table 5 presents the fitted log-logistic model for Conc_110mg, with ED50 as the parameter, using a four-parameter model. The slope parameter (b) is estimated at 2.8369 but is not statistically significant ($p = 0.0709$). The lower asymptote (c) is 1.2953 and is highly significant ($p = 0.0004$), indicating a strong effect at lower concentration levels. The upper asymptote (d) is 4.3268, also significant at the 0.01 level ($p = 0.0068$), suggesting a notable difference between lower and upper response limits. The ED50 parameter (e = 0.0351) is statistically significant at the 0.05 level ($p = 0.0225$), implying that the median effective concentration is well estimated. The residual standard error of 0.0846, with 3 degrees of freedom, suggests a reasonable fit of the model to the data.

Table 6-Comparative Analysis of Final Concentrations over Time at pH Levels 2 to 10

	pH_2	**pH_4**	**pH_6**	**pH_8**	**pH_{10}**
Time (mins)			Final Concentrations (mg/L)		
20	16.9392	4.5268	3.6610	3.610	1.6250
40	10.6969	2.2520	2.9431	1.9438	0.8830
60	8.7459	1.3525	1.7702	0.9330	0.6887
80	6.7515	0.8154	0.9210	0.6821	0.4893
100	5.5097	0.6231	0.5620	0.4122	0.3335
120	4.9276	0.5620	0.4822	0.3000	0.2110
160	4.8127	0.5531	0.4321	0.2696	0.1950
180	4.6825	0.5527	0.4220	0.2518	0.1800
340	4.6825	0.5527	0.4220	0.2518	0.1800

Table 6 presents a comparative analysis of final concentrations (mg/L) over time at varying pH levels (2 to 10). The results indicate a clear trend of decreasing final concentration over time across all pH levels, with the most rapid reduction occurring in alkaline conditions (pH 10). At 20 minutes, the highest concentration is observed at pH 2 (16.9392 mg/L), while the lowest is at pH 10 (1.6250 mg/L). As time progresses, this trend continues, with the final concentrations at 180 minutes stabilizing at 4.6825 mg/L for pH 2, 0.5527 mg/L for pH 4, 0.4220 mg/L for pH 6, 0.2518 mg/L for pH 8, and 0.1800 mg/L for pH 10. The data suggest that higher pH levels accelerate the reduction process, with minimal changes beyond 180 minutes, as concentrations remain constant for up to 340 minutes.

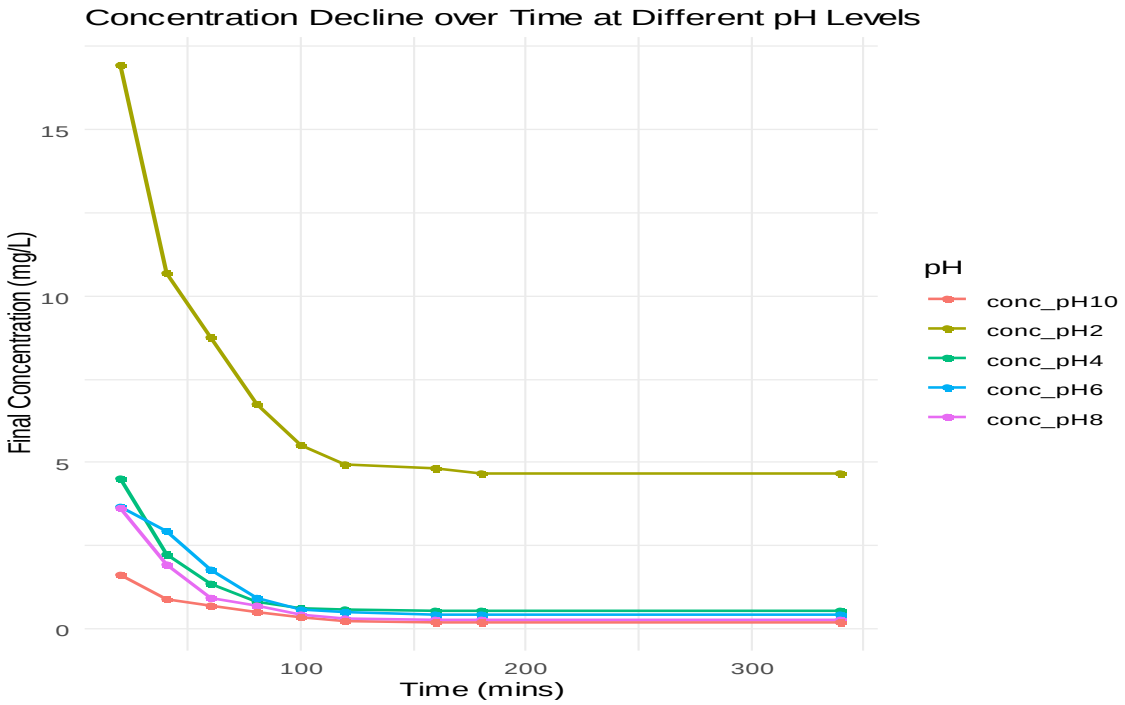

Fig. 3-Graph of concentration decline over time at different pH levels

Fig. 3 illustrates the decline in concentration over time at different pH levels (2, 4, 6, 8, and 10). The trend reveals that higher pH levels accelerate the reduction in concentration, with the most rapid decrease observed at pH 10. At 20 minutes, the concentration at pH 2 is highest (~16.94 mg/L), while pH 10 is lowest (~1.63 mg/L). As time progresses, concentrations across all pH levels decline, reaching near-stable values around 180 minutes, where pH 2 stabilizes at ~4.68 mg/L, pH 4 at ~0.55 mg/L, pH 6 at ~0.42 mg/L, pH 8 at ~0.25 mg/L, and pH 10 at ~0.18 mg/L. The results reinforce that higher alkalinity significantly enhances the degradation process, while acidic conditions slow it down.

Table 7. Summary for rate constants of the first-order decay model for each pH level

Source of Variation	**Estimate**	**Std.Error**	**t-value**	**p-value**
model_pH2$coefficients["k",]	0.0098	0.0023	4.2894	0.0036
model_pH4$coefficients["k",]	0.0271	0.0040	6.6981	0.0002
model_pH6$coefficients["k",]	0.0196	0.0023	8.3570	0.0000
model_pH8$coefficients["k",]	0.0292	0.0025	11.5139	0.0000
model_pH10$coefficients["k",]	0.0196	0.0023	8.5373	0.0000

Table 7 presents the rate constants (k) for the first-order decay model across different pH levels, highlighting significant variations in degradation rates. The highest decay rate is observed at pH 8 (k = 0.0292, $p < 0.0001$), followed closely by pH 4 (k = 0.0271, $p = 0.0002$), indicating faster degradation in mildly acidic and slightly alkaline conditions. Also, pH 2 exhibits the lowest decay rate (k = 0.0098, $p = 0.0036$), suggesting that strongly acidic conditions slow down the process. The rate constants for pH 6 and pH 10 are identical (k = 0.0196, $p < 0.0001$), implying moderate degradation efficiency in neutral and strongly alkaline environments. The consistently low *p*-values (< 0.01) confirm the statistical significance of these estimates, reinforcing the role of pH in influencing decay kinetics.

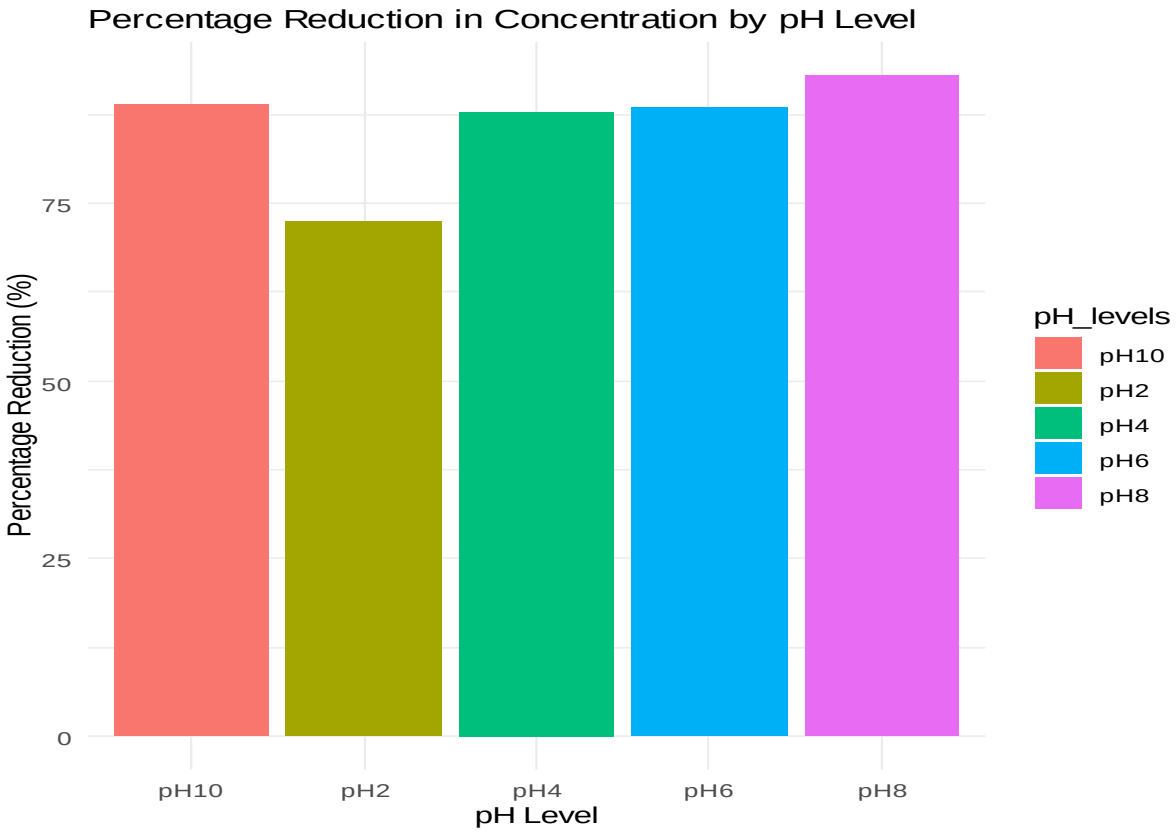

Fig. 4-Plot percentage reduction in concentration by pH level

Fig. 4 illustrates the percentage reduction in concentration across different pH levels, highlighting variations in degradation efficiency. The highest percentage reduction is observed at pH 8, followed closely by pH 10, pH 6, and pH 4, suggesting that degradation is more efficient in slightly alkaline conditions. Also, pH 2 exhibits the lowest percentage reduction, indicating that highly acidic environments slow down the degradation process. This trend aligns with the rate constant estimates in Table 7, where pH 8 had the highest decay rate (k = 0.0292, $p < 0.0001$), and pH 2 had the lowest (k = 0.0098, $p = 0.0036$). The error bars suggest some variability, but the general trend remains clear degradation is more effective at neutral to mildly alkaline pH levels than under strong acidic conditions.

6. Conclusions

This study evaluated the adsorption efficiency and dose-response behaviour of carbonized and potassium hydroxide (KOH)--activated hamburger seed shell (CPAHS) as a potential adsorbent for methylene blue dye removal from aqueous solutions. Through extensive characterization, including FTIR, SEM, and proximate analysis, the adsorbent demonstrated favourable physicochemical properties such as a high surface area (400.9–548.6 m^2/g), low ash content (3.2–6.0%), and significant fixed carbon content (88.5–89.7%), all of which contribute to its strong adsorption potential.

The adsorption performance of CPAHS was significantly influenced by pH, adsorbent dosage, and contact time. The results revealed that the removal efficiency was highest at near-neutral to slightly alkaline conditions (pH 6–8), where the positively charged methylene blue dye exhibited strong electrostatic interactions with the negatively charged functional groups on CPAHS. Extreme pH conditions (highly acidic or highly alkaline) resulted in reduced removal efficiency, likely due to protonation or charge repulsion effects.

Adsorbent dosage played a crucial role in optimizing dye removal, with increased CPAHS dosage leading to higher adsorption efficiency. However, beyond an optimal dosage threshold (0.15 g), diminishing returns were observed, suggesting that excessive dosage may lead to particle aggregation, reducing available active sites for adsorption. The dose-response analysis using a four-parameter log-logistic model provided a quantitative assessment of adsorption capacity, with key parameters such as ED50, upper

asymptote, and slope confirming the high efficiency of CPAHS. The kinetic modelling results indicated that the adsorption process followed a pseudo-second-order model, implying that chemisorption played a dominant role in dye removal. Furthermore, a first-order decay model was used to describe the rate of dye concentration reduction across varying pH conditions, with the fastest degradation observed at pH 6–8.

This study highlights the potential of hamburger seed shells, an agricultural waste material, as an effective, low-cost, and sustainable adsorbent for dye removal. Utilizing such biomass-based adsorbents provides an eco-friendly solution to both agricultural waste disposal and wastewater treatment challenges. The high adsorption efficiency and rapid dye removal capability of CPAHS make it a promising candidate for industrial wastewater treatment, particularly in textile and dyeing industries where methylene blue contamination is prevalent. Its ability to function effectively at neutral to slightly alkaline pH conditions also simplifies its integration into existing wastewater treatment systems without the need for extensive pH adjustments. The relatively simple preparation and activation process of CPAHS suggests its feasibility for large-scale production and application. Given the high availability of hamburger seed shells in regions where this plant is grown, the cost-effectiveness of this adsorbent makes it a competitive alternative to conventional activated carbons derived from expensive raw materials. The dose-response analysis and kinetic modelling provide a foundation for further optimizing CPAHS-based adsorption systems. Future research could explore modifications such as impregnation with metal oxides or hybrid composite materials to enhance adsorption capacity, selectivity, and regeneration potential. The study underscores the importance of developing low-impact, natural adsorbents for water purification, aligning with global sustainability goals. Given its efficiency in methylene blue dye removal, CPAHS may serve as a model for developing similar adsorbents for removing other pollutants, such as heavy metals and pharmaceuticals, from wastewater.

In conclusion, this study has demonstrated that CPAHS is an efficient and environmentally friendly adsorbent for methylene blue dye removal, with strong potential for industrial and environmental applications. By bridging the gap between waste valorization and water purification, this research contributes to the advancement of sustainable adsorption technologies, paving the way for greener and more cost-effective solutions in wastewater treatment.

Acknowledgement

None

References

[1] Mohammed, BA. Removal of Textile Dyes (Maxilon Blue, and Methyl Orange) by Date Stones Activated Carbon. *Int. J. Advan. Res. Chem. Sci.*, 2014, 1(1): 48-59.

[2] Ahmad, A, Mohd-Setapar, SH, Chuong, CS, Khatoon, A, Wani, WA, Kumar, R, Rafatullah, M. Recent advances in new generation dye removal technologies: novel search for approaches to reprocess wastewater. *RSC Advances*. 2015, 5(39), 30801-30818.

[3] Ertugay, N. and Acar, FN. Removal of COD and color from Direct Blue 71 azo dye wastewater by Fenton's oxidation: Kinetic study. Arabian Journal of Chemistry, 2017, 10, S1158-S1163.

[4] Mittal, A, Thakur, V, Mittal, J, Vardhan, H. Process development for the removal of hazardous anionic azo dye Congo red from wastewater by using hen feather as potential adsorbent. Desalination and Water Treatment, 2014, 52(1-3), 227-237.

[5] Bouasla, FI, and Samar, MEH. Effects of operator parameters, anions and cations on the degradation of AY99 in an aqueous solution using Fenton's reagent. Optimization and kinetics study. *Int. J. Ind. Chem*., 2012, vol. 3, pp. 1-11.

[6] Kyzas, GZ, Siafaka, PI, Pavlidou, EG, Chrissafis, KJ, Bikiaris, DN. Synthesis and adsorption application of succinyl-grafted chitosan for the simultaneous removal of zinc and cationic dye from binary hazardous mixtures. Chemical Engineering Journal, 2015, 259, 438-448.

[7] Bansal, RC, Donnet, JB, & Stoeckli, HF. Active carbon. Marcel Dekker, 1988, New York.

[8] Villet, VB M. The regeneration of activated carbon. Journal of the southern African institute of mining and metallurgy, 1991, 91(5): 159-167.

[9] Aljeboree, AM, Alshirifi, AN, Alkaim, AF. Kinetics and equilibrium study for the adsorption of textile dyes on coconut shell activated carbon. Arabian journal of chemistry, 2017, 10, S3381-S3393

[10] Alshabanat, M, Alsenani, G, and Almufarij, R. Research Article Removal of Crystal Violet Dye from Aqueous Solutions onto Date Palm Fiber. Chemistry, 2013, 9:1-6.

[11] Ajala, LO, Ali, EE, Obasi, NA, Fasuan, TO, Odewale, IO, Igidi, JO, & Singh, J. Insights into purification of contaminated water with activated charcoal derived from hamburger seed coat. *International Journal of Environmental Science and Technology*, 2022, 19(7), 6541–6554. https://doi.org/10.1007/s13762-021-03577-8

[12] Beksissa, R, Tekola, B, Ayala, T, & Dame, B. Investigation of the adsorption performance of acid treated lignite coal for Cr (VI) removal from aqueous solution. Environmental Challenges, 2021, 4. https://doi.org/10.1016/j.envc.2021.100091

[13] Aragaw, T A, & Alene, AN. A comparative study of acidic, basic, and reactive dyes adsorption from aqueous solution onto kaolin adsorbent: Effect of operating parameters, isotherms, kinetics, and thermodynamics. Emerging Contaminants, 2022, 8, 59–74. https://doi.org/10.1016/j.emcon.2022.01.002

[14] Bin-Dahman, OA, & Saleh, TA. Synthesis of polyamide grafted on biosupport as polymeric adsorbents for the removal of dye and metal ions. Biomass Conversion and Biorefinery, 2024, 14(2), 2439–2452. https://doi.org/10.1007/s13399-022-02382-8

[15] Rajoriya, S, Saharan, VK, Pundir, AS, Nigam, M, & Roy, K. Adsorption of methyl red dye from aqueous solution onto eggshell waste material: Kinetics, isotherms and thermodynamic studies. *Current Research in Green and Sustainable Chemistry*, 2021, 4. https://doi.org/10.1016/j.crgsc.2021.100180

[16] Rosly, NZ, Abdullah, AH, Kamarudin, MA, Ashari, SE, & Alang Ahmad, SA. Adsorption of methylene blue dye by calix[6]arene-modified lead sulphide (Pbs): Optimisation using response surface methodology. International Journal of Environmental Research and Public Health, 2021, 18(2), 1–20. https://doi.org/10.3390/ijerph18020397

[17] Tan, IAW, Hameed, BH, & Ahmad, AL. Equilibrium and kinetic studies on basic dye adsorption by oil palm fibre activated carbon. Chemical Engineering Journal, 2007, 127: 111–119.

[18] Nwabanne, JT, and Mordi, MI. Equilibrium uptake and sorption dynamics for the removal of a basic dye using bamboo. African Journal of Biotechnology, 2009, 8 (8): 1555-1559.

[19] Foo, KY and Hameed, BH. Microwave- assisted regeneration of activated carbon. Bioresource Technology, 2012, 119: 234-240.

[20] Mall, ID, Srivastava, VC, & Agarwal, NK. Removal of orange- G and methyl violet dyes by adsorption onto bagasse fly ash, Kinetics study and equilibrium isotherm analyses. Dyes pigments, 2006, 69: 210-223.

[21] Rengaraj, S, Seung –Hyeon, M, & Sivabalm, S. Agricultural solid waste for the removal of organic adsorption of phenol from waste and waste water by palm seed coat activated carbon. Waste Management, 2012, 22: 543-548.

[22] Azubike, CP, Rodriguez, H, Okhamafe, AO, & Rogers, RD. Physicochemical properties of maize cob cellulose powder reconstituted from ionic liquid solution. Cellulose, 2012, 19(8): 425-433.